Wild-Type Levels of Nuclear Localization and Human Immunodeficiency Virus Type 1 Replication in the Absence of the Central DNA Flap

JOURNAL OF VIROLOGY, Dec. 2002, p. 12078–12086 Vol. 76, No. 23
0022-538X/02/$04.00+0 DOI: 10.1128/JVI.76.23.12078–12086.2002

Wild-Type Levels of Nuclear Localization and Human Immunodeficiency Virus Type 1 Replication in the Absence of the Central DNA Flap

Ana Limón, Noriko Nakajima,† Richard Lu, Hina Z. Ghory, and Alan Engelman*

Department of Cancer Immunology and AIDS, Dana-Farber Cancer Institute, and Department of Pathology, Harvard Medical School, Boston, Massachusetts 02115

Received 19 February 2002/Accepted 27 August 2002

Numerous factors have been implicated in the nuclear localization of retroviral preintegration complexes. Whereas sequences in human immunodeficiency virus type 1 (HIV-1) matrix, Vpr, and integrase proteins were initially reported to function specifically in nondividing cells, other recently identified sequences apparently function in dividing cells as well. One of these, the central DNA flap formed during reverse transcription, is specific to lentiviruses. It was previously reported that flap-negative (F^-) HIV-1_{LAI} was completely defective for viral spread in the MT-4 T-cell line, yet F^- HIV-1 vectors were only 2- to 10-fold defective in various single-round transduction assays. To address these different findings, we analyzed the infectivity and nuclear localization phenotypes of two highly related T-cell-tropic strains, HIV-1_{NL4-3} and a derivative of HIV-1_{HXBc2} deficient for both Vpr and Nef. In stark contrast to the previous report, F^- derivatives of both strains replicated efficiently in MT-4 cells. F^- HIV-1_{NL4-3} also spread like wild-type HIV-1_{NL4-3} in infected Jurkat and primary T-cell cultures. In contrast, F^- HIV-1_{HXBc2} was replication defective in primary T cells. Results of real-time quantitative PCR assays, however, indicated that F^- HIV-1_{HXBc2} entered primary T-cell nuclei as efficiently as its wild-type counterpart. Thus, the F^- HIV-1_{HXBc2} growth defect did not appear to correlate with defective nuclear import. Consistent with this observation, wild-type *nef* restored replication to F^- HIV-1_{HXBc2} in primary T cells. Our results indicate that the central DNA flap does not play a major role in either preintegration complex nuclear import or HIV-1 replication in a variety of cell types.

Two enzymes, reverse transcriptase (RT) and integrase, carry out essential tasks during the early phase of the retroviral life cycle. Soon after entry, RT copies viral RNA into linear double-stranded cDNA. The integrase then catalyzes the insertion of this cDNA into a cell chromosome. Reverse transcription and integration take place in the context of large nucleoprotein complexes called reverse transcription complexes and preintegration complexes, respectively (reviewed in reference 22).

Retroviral preintegration complexes must enter cell nuclei, where the chromosomal targets of integration reside. The nuclear envelope contains numerous nuclear pore complexes, which regulate the transport of macromolecules into and out of the nucleus. Nuclear pore complexes permit passive diffusion of macromolecules with diameters of less than about 9 nm, equating to proteins in the 40- to 60-kDa range (reviewed in reference 34). The size of human immunodeficiency virus type 1 (HIV-1) and Moloney murine leukemia virus preintegration complexes, estimated to be near or greater than the size of the eukaryotic ribosome (3, 18), precludes their passive transport through nuclear pore complexes (reviewed in references 21 and 22).

Lentiviruses like HIV-1 productively infect nondividing target cells (6, 33, 47). In contrast, Moloney murine leukemia virus requires cell division to establish a productive infection (24, 32, 43). Whereas HIV-1 enters nondividing cell nuclei by an energy-dependent process (6), Moloney murine leukemia virus requires the dissociation of nuclear membranes during mitosis, which in theory leads to preintegration complex-chromosome interactions in the absence of active transport (32, 43). One interpretation of these results is that HIV-1 preintegration complexes contain nuclear localization signals that govern their active transport through intact nuclear pore complexes, and Moloney murine leukemia virus fails to infect nondividing cells due to the lack of appropriate signals (21, 22).

Recently, replication-defective Moloney murine leukemia virus (49) and HIV-1 (2, 50) mutants were identified as being blocked at the nuclear import step in dividing target cells. This suggested that retroviral preintegration complexes might interact with specific host cell factors to achieve nuclear localization even in cells that are actively dividing (15). One of the two HIV-1 factors implicated in this novel type of nuclear localization is the *cis*-acting central DNA flap formed during reverse transcription (50). The flap is a 99-base overlap of the plus-strand formed by the central polypurine tract (cPPT) and central termination sequence (8–10, 50). Flap-negative (F^-) strain HIV-1_{LAI} was replication defective in peripheral blood mononuclear cells (PBMC) and the MT-4 T-cell line (50). The complete replication block in MT-4 cells suggested that F^- HIV-1_{LAI} was at least 10^4-fold defective in its ability to initiate a spreading viral infection (37, 50).

* Corresponding author. Mailing address: Department of Cancer Immunology and AIDS, Dana-Farber Cancer Institute, 44 Binney St., Boston, MA 02115. Phone: (617) 632-4361. Fax: (617) 632-3113. E-mail: alan_engelman@dfci.harvard.edu.

† Present address: Department of Pathology, National Institute of Infectious Diseases, Shinjuku-ku, Tokyo 162-8640, Japan.

One model for the flap in HIV-1 replication was that it allowed preintegration complexes to adopt a folded structure required for efficient transport through nuclear pore complexes (50). This model was based on the central location of the flap in the HIV-1 genome, which in two dimensions places it diametrically opposed to the integrase-containing intasome that synapses the two ends of the retroviral cDNA together and mediates integration (11, 12, 46). In contrast to the results with replication-competent HIV-1, F^- viral vectors were only 2- to 10-fold defective in single-round infection assays (16, 20, 39, 40, 44, 50, 51). Because of this, it was suggested that the smaller size of vector genomes precluded the absolute requirement for the flap during nuclear import (50).

In this study, we investigated the role of the flap in preintegration complex nuclear import by analyzing the infectivity and nuclear localization of two different HIV-1 strains. Our results show that the flap is not required for efficient HIV-1 spread and preintegration complex nuclear import in a variety of cell types.

MATERIALS AND METHODS

Plasmids. The cPPT-D mutation (50) was introduced into pNL43/*Xma*I (4) and pHXBH10-vpu$^+$ (23), encoding wild-type HIV-1_{NL4-3} (1) and a Vpu-positive derivative of HIV-1_{HXBc2} (19), respectively, by PCR mutagenesis (17, 37). The presence of desired base changes as well as the absence of off-site changes was confirmed by DNA sequencing. To generate a Nef$^+$ F^- derivative of HIV-1_{HXBc2}, the 1.8-kb *Pfl*M-I fragment from F^- pHXBH10-vpu$^+$ was swapped for the corresponding fragment in pHXB/Nef$^+$ (5).

Plasmid pHXBH10ΔenvCAT-vpu$^+$ (42) encoded envelope (Env)-deleted (Env$^-$) HIV-1_{HXBc2} carrying the bacterial chloramphenicol acetyltransferase (CAT) gene in the viral *nef* position. Env$^-$ F^- HIV-1_{HXBc2} was made by swapping the 1.8-kb *Pfl*M-I fragment from F^- pHXBH10-vpu$^+$ for the corresponding fragment in pHXBH10ΔenvCAT-vpu$^+$. Plasmid pNLXΔenv was made by digesting pNL43/*Xma*I with *Nhe*I and *Stu*I, treating with Klenow fragment, and religating. Plasmid pNLXΔenvCAT was made by exchanging the CAT gene for *nef* region nucleotides 8785 to 9017 (1, 35). F^- pNLXΔenv and F^- pNLXΔenvCAT were made by swapping the 1.8-kb *Age*I-*Pfl*M-I fragment from F^- pNL43/*Xma*I for the corresponding fragments in pNLXΔenv and pNLXΔenvCAT, respectively.

Env expression vectors pSVIII-env (25) and pHCMV-G (48) encoded HIV-1_{HXBc2} and vesicular stomatitis virus G (VSV-G) glycoproteins, respectively. An HIV-1_{NL4-3} Env expression vector was made by swapping the 2.1-kb *Kpn*I-*Bam*HI fragment from pNL43/*Xma*I for the corresponding pSVIII-env fragment. The resulting pNLXE7 plasmid encoded a chimeric Env with amino acid residues 42 to 750, comprising most of gp120 and gp41, derived from HIV-1_{NL4-3}.

Plasmid pUC19.2LTR was built by amplifying Hirt supernatant from HIV-1_{NL4-3}-infected CEM-12D7 cells (37) with *Eco*RI-tagged primer AE761 (5′-ACTGACGAATTCGAGCTTGCTACAAGG-3′) and *Bam*HI-tagged AE762 (5′-CATGCAGGATCCCAGGGTGTAACAAGCTGG-3′), digestion, and ligation to *Eco*RI- and *Bam*HI-digested pUC19.

Cells, viruses, and infections. Virus stocks for replication assays were prepared by transfecting 293T cells with calcium phosphate as described previously (17, 37). Single-round viruses for real-time quantitative (RQ)-PCR and in vitro CAT assays were prepared by transfecting 293T cells with FuGENE 6 (Roche Molecular Biochemicals, Indianapolis, Ind.) and treating the filtered supernatants with DNase I as described previously (12). Viruses were counted with an exogenous ^{32}P-based RT assay (17, 37).

Activated PBMC were prepared from human blood as described previously (37). PBMC, Jurkat cells, and MT-4 cells (2×10^6) were infected with equal RT counts per minute (cpm) of wild-type and mutant virus for spreading infection assays essentially as described previously (37). For in vitro CAT assays, cells (2×10^6) were infected with 5×10^6 RT cpm of HIV-1 pseudotypes. In vitro CAT activity was determined as previously described (37).

For RQ-PCR assays, cells (6×10^6) were infected with 6×10^6 RT cpm of HIV-1_{NL4-3} or 3×10^7 to 6×10^7 RT cpm of HIV-1_{HXB2} pseudotypes by spinoculation (38) at $480 \times g$ for 2 h. For Southern blotting, SupT1 cells (2×10^7) were infected with 10 ml of DNase I-treated HIV-1_{NL4-3} essentially as described previously (12), and MT-4 cells (2×10^6) were infected with 10^7 RT cpm of HIV-1_{HXBc2} by spinoculation. All infection assays were performed a minimum of two times.

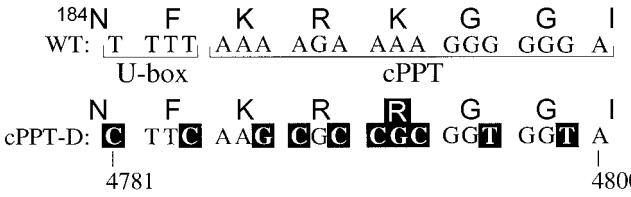

FIG. 1. Wild-type and mutant sequences. The central U-box and cPPT form part of the integrase coding region. Mutant sequences that differ from the wild-type (WT) sequence are highlighted by black boxes. Note that the cPPT-D mutation substitutes Arg for Lys-188 in the integrase. This change alone does not appear to impact integrase function, as HIV-1_{LAI} carrying just the K188R change replicated like the wild-type virus under conditions in which the HIV-1_{LAI} cPPT-D mutant was replication defective (50). Numbering is that for HIV-1_{NL4-3} (1, 35).

Flap detection assay. HIV-1_{NL4-3} cDNA was purified from SupT1 cell (2×10^7) cytoplasmic extracts (0.5 ml) prepared at 7 h postinfection essentially as described previously (12). HIV-1_{HXBc2} cDNA was purified from Hirt supernatant fractions of MT-4 cells (4×10^6) lysed (37) 2 to 3 days postinfection. Purified cDNA was treated with S1 nuclease (1.5 U/μg of total DNA) (Amersham Pharmacia Biotech Inc., Piscataway, N.J.) for 30 min at 37°C (27). The minus strand of HIV-1 was detected by Southern blotting with a *nef*/U3-specific riboprobe as described previously (4, 12).

RQ-PCR assays. DNA from infected cells was extracted with the DNeasy tissue kit as recommended by the manufacturer (Qiagen, Valencia, Calif.). DNA concentration was determined spectrophotometrically, and equal levels of total cellular DNA (250 ng or 500 ng) were analyzed by RQ-PCR essentially as described previously (7, 13, 29, 31). Infections were performed in duplicate, and each infection was analyzed in duplicate by RQ-PCR. Virus particles lacking Env glycoprotein were used in most infections to control for plasmid DNA carryover from transfections.

HIV-1 primers, probes, and PCR conditions were as previously described (7) except that the minus-strand primer for late reverse transcription HIV-1_{NL4-3} products was AE331 (5′-CCTGCGTCGAGAGATCTCCTCTGG-3′). Plasmids p83-2/*Xma*I and pSVC21/5′-LTR (4) were used to generate standard curves for HIV-1_{NL4-3} and HIV-1_{HXBc2} late reverse transcription products, respectively. Plasmid pUC19.2LTR was used as the standard for the two-long-terminal-repeat (2-LTR)-containing HIV-1 circle.

RESULTS

F^- HIV-1_{NL4-3} displays wild-type replication kinetics under a variety of infection conditions. Retroviral polypurine tracts are preceded by an upstream uridine-rich sequence known as the U-box (28), and a 4-base U-box abuts the 16-bp HIV-1 cPPT (Fig. 1). The cPPT-D mutation, which replaced two U-box bases with cytosine and replaced 6 of the 16 purines with pyrimidines (Fig. 1), inhibited synthesis of the central DNA flap during reverse transcription of HIV-1_{LAI} (50). The resulting F^- mutant was unable to initiate a spreading infection in either PBMC or MT-4 cells (50). We found it surprising that F^- HIV-1_{LAI}, which expressed a functional integrase protein (Fig. 1), was unable to initiate a spreading infection in MT-4 cells because we recently reported that HIV-1_{NL4-3} lacking functional integrase replicated in these cells, albeit delayed approximately 1 week compared with the wild-type (37). Because of the complete block in MT-4 cells, we inferred that F^- HIV-1_{LAI} was at least 10^4-fold defective in its ability to initiate a spreading viral infection (37, 50). In contrast to this large defect in viral spread, F^- HIV-1 vectors were only 2- to 10-fold

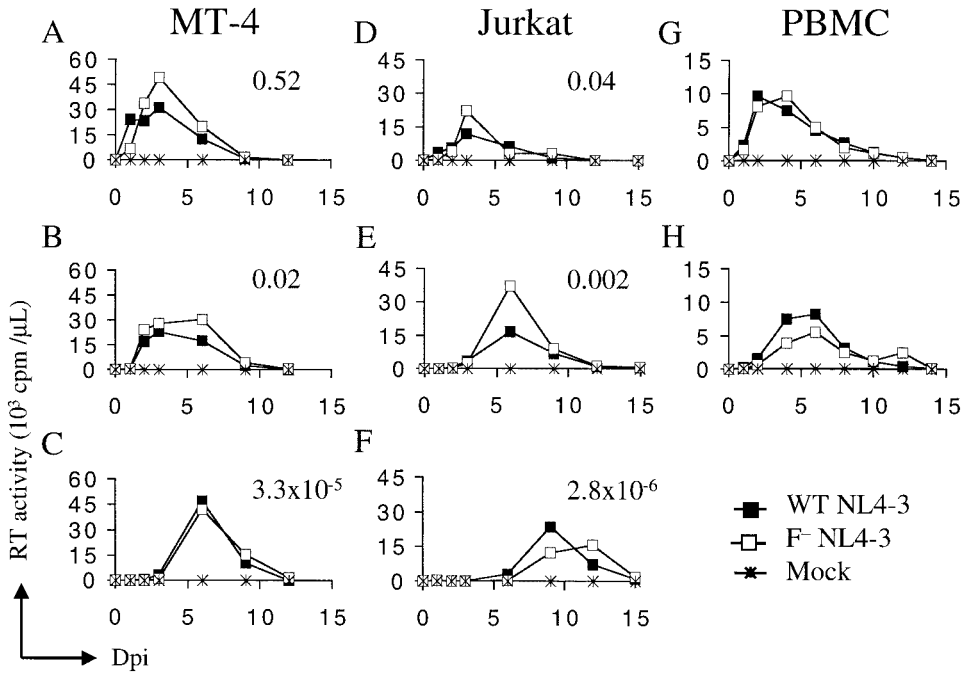

FIG. 2. F⁻ HIV-1_{NL4-3} displays wild-type replication kinetics. (A) MT-4 cells infected with 10^6 RT cpm of wild-type (WT) HIV-1_{NL4-3} (■), F⁻ HIV-1_{NL4-3} (□), or supernatant from mock-transfected cells (×). (B) MT-4 cells infected with 4×10^4 RT cpm of the viruses indicated in panel A. (C) MT-4 cells infected with 64 RT cpm of virus. (D through F) Jurkat cells infected with the levels of wild-type and F⁻ viruses indicated for MT-4 cells in panels A to C, respectively. (G and H) PBMC infected with 10^6 and 4×10^4 RT cpm, respectively, of the indicated viruses. Numbers in panels A though F are multiplicities of infection for wild-type HIV-1_{NL4-3} based on previously reported $TCID_{50}$ values (37). Dpi, days postinfection.

defective in single-round infectivity assays (16, 20, 39, 40, 44, 50, 51).

To further investigate the role of the flap in HIV-1 infection, the cPPT-D mutation was introduced into two related T-cell-tropic strains, HIV-1_{NL4-3} and HIV-1_{HXBc2} (1, 19, 35). HIV-1_{NL4-3} is a chimera of HIV-$1_{NY5'}$ and HIV-1_{LAI} (1). Because HIV-1_{LAI} is highly related to HIV-1_{HXB2} (35), HIV-1_{NL4-3} and HIV-1_{HXBc2} are most related in their 3′ halves; the strains are 96.7% and 98.5% identical upstream and downstream of the *Eco*RI site that determined the chimera junction in HIV-1_{NL4-3}, respectively (1, 19, 35). HIV-1_{NL4-3} and HIV-1_{HXBc2} differ in the functionality of accessory gene products. Whereas all genes in HIV-1_{NL4-3} (1) and HIV-1_{LAI} (41) are intact, the HIV-1_{HXBc2} strain used in the majority of the spreading replication assays here was defective for *vpr* and *nef* (19, 23).

Since it was determined that F⁻ HIV-1_{LAI} was completely defective in MT-4 cells (50), we first assayed wild-type and F⁻ virus replication in MT-4 cells infected at a relatively high multiplicity of infection (MOI). Cells infected with 10^6 RT cpm of wild-type HIV-1_{NL4-3}, which equated to an MOI of approximately 0.5 (37), supported peak virus replication 3 days postinfection (Fig. 2A). Unexpectedly, F⁻ HIV-1_{NL4-3} displayed the wild-type replication profile (Fig. 2A). Diluting virus 25-fold again yielded similar wild-type and F⁻ replication kinetics in MT-4 cells (Fig. 2B). A further 625-fold dilution, equating to an MOI of just 3.3×10^{-5}, again yielded identical replication profiles for the wild-type and F⁻ HIV-1_{NL4-3} viruses (Fig. 2C). We note that on average, only 65 virions initiated infection under these conditions (37).

Since Jurkat cells were approximately 11-fold less permissive than MT-4 cells in their ability to replicate HIV-1_{NL4-3} (37), we next analyzed wild-type and F⁻ virus replication in Jurkat cells to see if a defective F⁻ phenotype might be visible under these somewhat more stringent growth conditions. Jurkat cells infected with 10^6 and 4×10^4 RT cpm, which correlated to approximate MOIs of 0.04 and 0.002, respectively (37), supported very similar replication profiles for the wild-type and F⁻ HIV-1_{NL4-3} viruses (Fig. 2D and E). Jurkat cells infected at an MOI of 2.8×10^{-6} supported peak wild-type HIV-1_{NL4-3} replication 9 days postinfection (Fig. 2F). In this case, the growth of F⁻ HIV-1_{NL4-3} was delayed approximately 3 days compared with the wild-type virus (Fig. 2F). Under these conditions, only about six wild-type virions initiated infection.

Wild-type and F⁻ HIV-1_{NL4-3} virus replication was also tested in primary human PBMC. PBMC infected with 10^6 and 4×10^4 RT cpm once again supported very similar profiles of wild-type and F⁻ HIV-1_{NL4-3} replication (Fig. 2G and H). We note that the precise MOIs for these infections are unknown because we have not determined 50% tissue culture infectious doses ($TCID_{50}$) with PBMC. Nonetheless, we conclude that an intact cPPT sequence confers very little if any growth advantage on HIV-1_{NL4-3} under a variety of conditions of viral spread (Fig. 2).

HIV-1_{HXBc2} cPPT-D mutant is replication defective in primary T cells. We next analyzed the replication profiles of the wild-type and F⁻ HIV-1_{HXBc2} viruses under the infection conditions described for Fig. 2. In this case, precise MOIs were unknown, as we did not determine HIV-1_{HXBc2} titers by

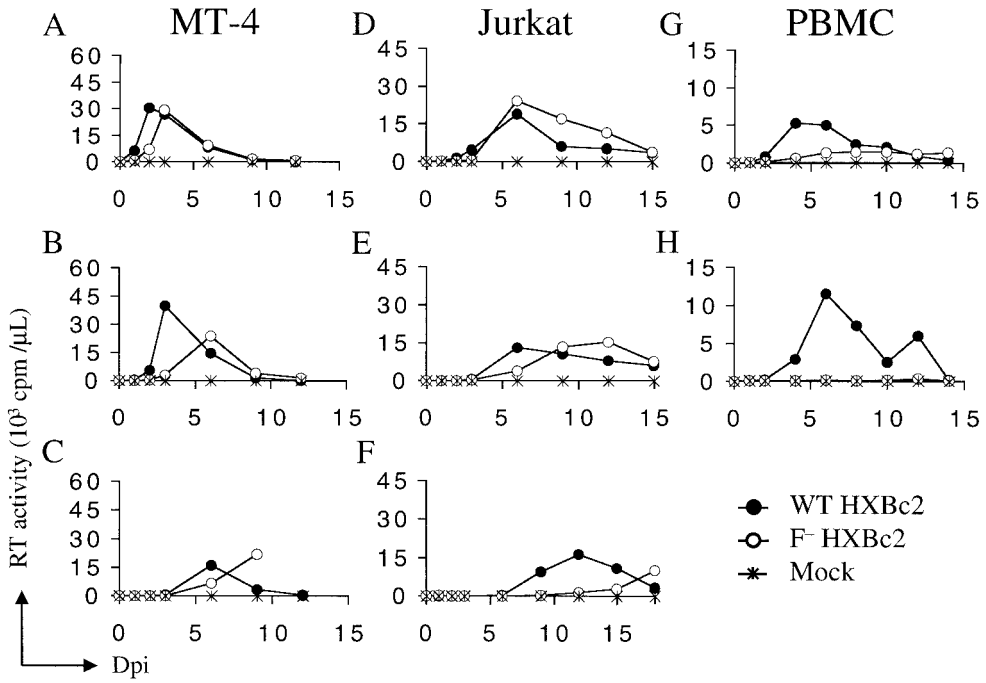

FIG. 3. F⁻ HIV-1_{HXBc2} displays a target cell type-dependent replication defect. Cells in panels A though H were infected with the same levels of wild-type (WT, ●) and F⁻ (○) HIV-1_{HXBc2} RT cpm as indicated for HIV-1_{NL4-3} in Fig. 2, panels A to H. Other labeling is the same as in Fig. 2.

$TCID_{50}$. MT-4 cells infected with 10^6 RT cpm of wild-type HIV-1_{HXBc2} supported peak virus replication 2 days postinfection, and F⁻ HIV-1_{HXBc2} replicated with an apparent 1-day delay under these conditions (Fig. 3A). Diluting HIV-1_{HXBc2} prior to infection revealed a subtle replication defect: the F⁻ virus was delayed about 3 days compared with the wild-type virus in cells infected with 4×10^4 and 64 RT cpm (Fig. 3B and C).

The slight defect observed in MT-4 cells was enhanced in less permissive Jurkat cells and PBMC. Jurkat cells infected with 10^6 RT cpm supported similar replication profiles of the wild-type and F⁻ HIV-1_{HXBc2} viruses (Fig. 3D). However, F⁻ HIV-1_{HXBc2} growth was delayed about 6 days compared with the wild-type virus following infection with 4×10^4 RT cpm (Fig. 3E) and 64 RT cpm (Fig. 3F). Most notably, F⁻ HIV-1_{HXBc2} was almost completely replication defective in PBMC (Fig. 3G and H). Whereas PBMC infected with 10^6 RT cpm supported weak F⁻ HIV-1_{HXBc2} growth (Fig. 3G), replication was barely detected following infection with 4×10^4 RT cpm in repeated experiments (Fig. 3H). Unlike the results obtained with HIV-1_{NL4-3}, we conclude that the cPPT-D mutation can alter the replication profile of HIV-1_{HXBc2}. However, the ability to detect a complete replication defect depended on MOI and target cell type (Fig. 3).

Wild-type levels of HIV-1 replication in the absence of the central DNA flap. The results of the previous experiments revealed the cPPT-D mutation differentially affected the replication capacities of HIV-1_{HXBc2} and HIV-1_{NL4-3}. Whereas F⁻ HIV-1_{NL4-3} displayed wild-type replication kinetics under a variety of conditions (Fig. 2), 4×10^4 RT cpm of F⁻ HIV-1_{HXBc2} failed to initiate a spreading infection in PBMC (Fig. 3). Because of this, we considered the possibility that the cPPT-D mutation might differentially affect the synthesis of the central DNA flap in the two strains. Although this seemed unlikely because the cPPT and central termination sequence lie in a region that is highly conserved between HIV-1_{LAI}, HIV-1_{HXBc2}, and HIV-1_{NL4-3} (1, 19, 35, 41), we nonetheless characterized wild-type and F⁻ HIV-1_{NL4-3} and HIV-1_{HXBc2} cDNAs purified from infected cells to address the possibility of differential flap DNA synthesis.

The flap detection assay (Fig. 4A) was based on previous observations that HIV-1 contains a hypersensitive site for S1 nuclease near the middle of the minus strand (9, 26). The flap is a 99-base overlap of the lentiviral plus strand, and this plus strand discontinuity yields the minus-strand cleavage site (Fig. 4A). Southern blots were probed with a riboprobe complementary to the downstream region of the minus strand. In this way, wild-type cDNA should yield a 4.9-kb minus-strand S1 digestion product. F⁻ digests, in contrast, should lack this product (Fig. 4A).

Similar levels of full-length minus-strand wild-type and F⁻ HIV-1_{NL4-3} cDNAs were synthesized in the cytoplasm of acutely infected SupT1 cells (Fig. 4B, lanes 1 and 2). Digestion with S1 nuclease yielded a readily detectable 4.9-kb wild-type product (Fig. 4B, lane 4) that was absent from the F⁻ digest (Fig. 4B, lane 5). Thus, as predicted, the cPPT-D mutation abolished the centrally located S1-hypersensitive site in the HIV-1_{NL4-3} minus strand and, by extension, the synthesis of the central DNA flap. We noted, however, the appearance of several novel bands in the F⁻ HIV-1_{NL4-3} digest (Fig. 4B, lane 5). The potential significance of these minor cleavage products is addressed in the Discussion.

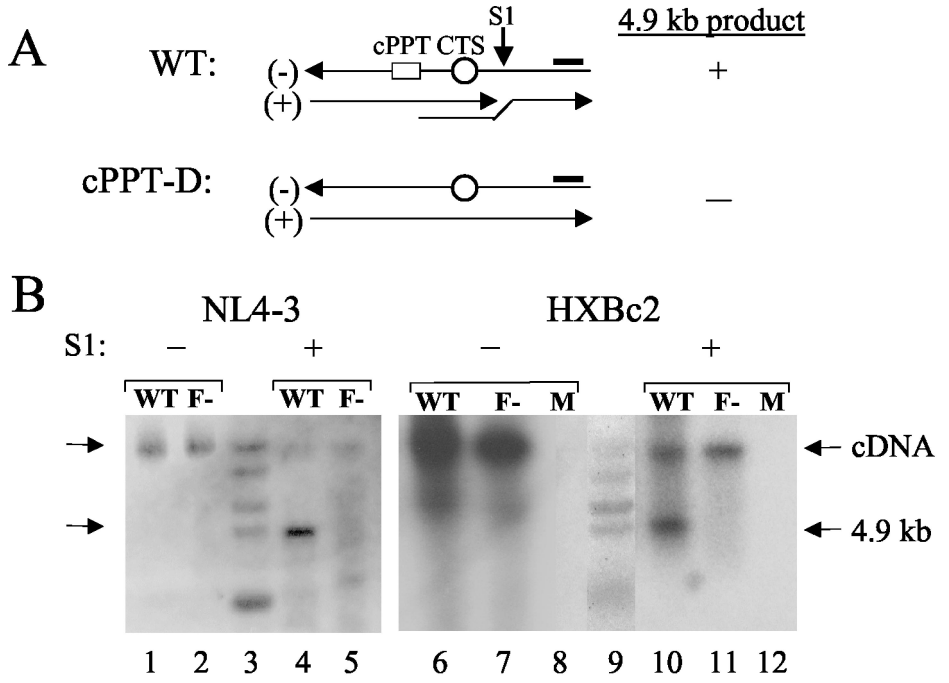

FIG. 4. cPPT-D mutation inhibits synthesis of the central DNA flap in HIV-1_{NL4-3} and HIV-1_{HXBc2}. (A) Flap detection assay. The predicted structures of the plus and minus strands in the central region of wild-type (WT) and cPPT-D mutant cDNAs are shown. The discontinuous wild-type plus strand yields the minus-strand S1 nuclease-sensitive site. The thick line indicates the relative position of the minus-strand-specific riboprobe. CTS, central termination sequence. (B) Southern blot. Purified cDNAs were either digested with S1 nuclease or left untreated, as indicated. The migration positions of the full-length and half-genome minus strands are marked cDNA and 4.9 kb, respectively. Molecular mass standards were loaded in lanes 3 and 9. M, lysate prepared from mock-infected cells.

SupT1 cells infected with the wild-type and F^- HIV-1_{HXBc2} viruses yielded barely detectable levels of cytosolic cDNA synthesis. To circumvent this, infected MT-4 cells were propagated for 2 to 3 days to allow viral spread and cDNA amplification, and total cell lysates were prepared by the Hirt method. The wild-type and F^- HIV-1_{HXBc2} viruses yielded similar levels of cDNA synthesis under these conditions (Fig. 4B, lanes 6 and 7). As witnessed for HIV-1_{NL4-3}, S1-digested wild-type HIV-1_{HXBc2} yielded a subgenomic 4.9-kb product that was absent from the F^- digest (Fig. 4B, lanes 10 and 11). Thus, as predicted, the cPPT-D mutation effectively inhibited the synthesis of the HIV-1_{HXBc2} flap.

F^- mutants are at most twofold defective for nuclear import. We next analyzed the role of the flap in the nuclear localization of HIV-1_{NL4-3} and HIV-1_{HXBc2} cDNA. The linear duplex product of reverse transcription is the cDNA substrate for integrase-mediated integration into chromosomal DNA (reviewed in references 14 and 22). In addition to integrated proviruses, unintegrated linears are converted into 1- and 2-LTR-containing DNA circles in the nuclei of infected cells (14, 21, 22). The 2-LTR circle has been used extensively as a marker for nuclear localization because the LTR-LTR circle junction affords a unique sequence for PCR amplification (14).

In this study, we used RQ-PCR to quantify levels of total HIV-1 and 2-LTR circles in single-round infections and used the fraction of 2-LTR circles as an indicator of preintegration complex nuclear import. Although this technique did not account for total nuclear HIV-1 DNA, it nonetheless afforded quantitative comparison of wild-type and mutant nuclear import activities. Env^- derivatives of HIV-1_{NL4-3} and HIV-1_{HXBc2} were used in RQ-PCR assays to restrict reverse transcription and nuclear import to single-round infections.

Jurkat cells infected with HIV-1_{NL4-3} supported similar levels of wild-type and F^- cDNA synthesis in repeated experiments (Fig. 5A and data not shown). By 24 h postinfection, 0.7% to 0.9% of wild-type cDNA was present as 2-LTR circles (Fig. 5A and B and data not shown). In four different experiments, the fraction of F^- HIV-1_{NL4-3} circles ranged from 48% to 89% of the wild-type value (Fig. 5A and B and data not shown), with an average value of 63% ± 16.2%. Thus, the flap affected HIV-1_{NL4-3} 2-LTR circle formation at most twofold under these assay conditions.

Wild-type HIV-1_{HXBc2} yielded only 10% to 20% of the level of wild-type HIV-1_{NL4-3} cDNA under identical infection conditions (data not shown). To improve on this relatively low cDNA yield, the apparent MOI was increased 10-fold by (i) increasing the level of virus inoculum fivefold and (ii) analyzing twice as much total cellular DNA by RQ-PCR. In repeated experiments, Jurkat cells supported three- to fivefold less F^- HIV-1_{HXBc2} cDNA synthesis than wild type, and F^- HIV-1_{HXBc2} formed about half as many 2-LTR circles as the wild type did (Fig. 6A and B and data not shown). However, due to the lower amount of total cDNA synthesis, the fraction of F^- HIV-1_{HXBc2} cDNA converted into 2-LTR circles actually exceeded the wild-type value in repeated experiments (Fig. 6A and B; Table 1).

Since the flap was more important for efficient spread in PBMC than in Jurkat cells (Fig. 3), we next analyzed F^-

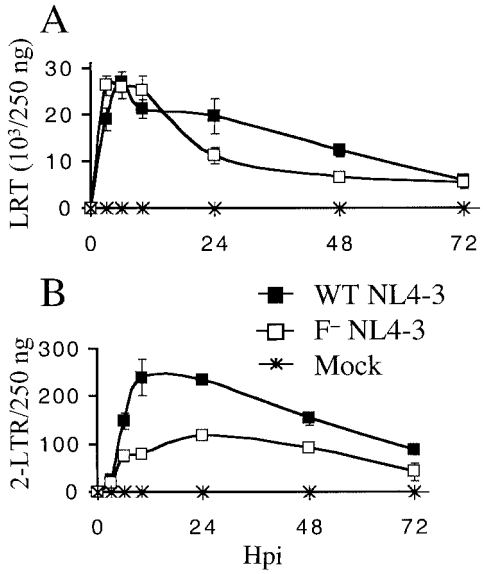

FIG. 5. cPPT-D mutation reduces the formation of HIV-1_{NL4-3} 2-LTR circles approximately twofold in Jurkat cells. (A) Cells infected with wild-type (WT) HIV-1_{NL4-3} (■), F⁻ HIV-1_{NL4-3} (□), or supernatant from Env⁻ transfections (×) were lysed at the indicated times, and 250 ng of total cellular DNA was assayed for total HIV-1 cDNA by RQ-PCR. (B) Cells infected with wild-type HIV-1_{NL4-3} (■), F⁻ HIV-1_{NL4-3} (□), or mock-treated supernatant (×) were analyzed for levels of 2-LTR circles by RQ-PCR. Error bars represent variations between duplicate RQ-PCR assays. LRT, late reverse transcription; Hpi, hours postinfection.

HIV-1_{HXBc2} cDNA synthesis and 2-LTR circle formation in PBMC. PBMC supported about twofold less F⁻ HIV-1_{HXBc2} than wild-type cDNA synthesis in repeated experiments (Fig. 6C and data not shown). Wild-type HIV-1_{HXBc2} converted only a minor fraction of its total cDNA into 2-LTR circles under these infection conditions (Fig. 6D). Although the fraction of total F⁻ HIV-1_{HXBc2} converted into 2-LTR circles was similar to that of the wild type (Fig. 6C and D; Table 1), infections were repeated with VSV-G pseudotypes in hopes of increasing the efficiencies of cDNA synthesis and 2-LTR circle formation.

TABLE 1. Nuclear import activity of F⁻ HIV-1_{HXBC2} in Jurkat cells and PBMC

Cells	Expt	2-LTR circle formation[a] (% of control) for infections mediated by:	
		HIV-1 Env	VSV-G
Jurkat	1	185[b]	112[c]
	2	274	249
PBMC	1	75[b]	113[c]
	2	192	93

[a] Expressed as a percentage of wild-type HIV-1_{HXBc2} 2-LTR circle formation relative to total cDNA synthesis.
[b] Experiment presented in Fig. 6.
[c] Data from Fig. 7.

As anticipated, VSV-G significantly enhanced wild-type HIV-1_{HXBc2} cDNA synthesis and 2-LTR circle formation in Jurkat cells (compare Fig. 7A and B with Fig. 6A and B). Wild-type and F⁻ HIV-1_{HXBc2} VSV-G pseudotypes synthesized similar cDNA levels in repeated experiments (Fig. 7A and data not shown). The flap did not appear to affect 2-LTR circle formation under these conditions, as similar levels of wild-type and F⁻ cDNA were converted into 2-LTR circles in repeated experiments (Fig. 7A and B; Table 1). PBMC infected with VSV-G pseudotypes also supported similar levels of wild-type and F⁻ HIV-1_{HXBc2} cDNA synthesis (Fig. 7C). And, in repeated experiments, both viruses formed similar levels of 2-LTR circles (Fig. 7C and D; Table 1).

Strain-dependent flap function. F⁻ HIV-1_{HXBc2} failed to replicate in PBMC (Fig. 3H) under conditions in which F⁻ HIV-1_{NL4-3} replication was readily detected (Fig. 2H). Yet the

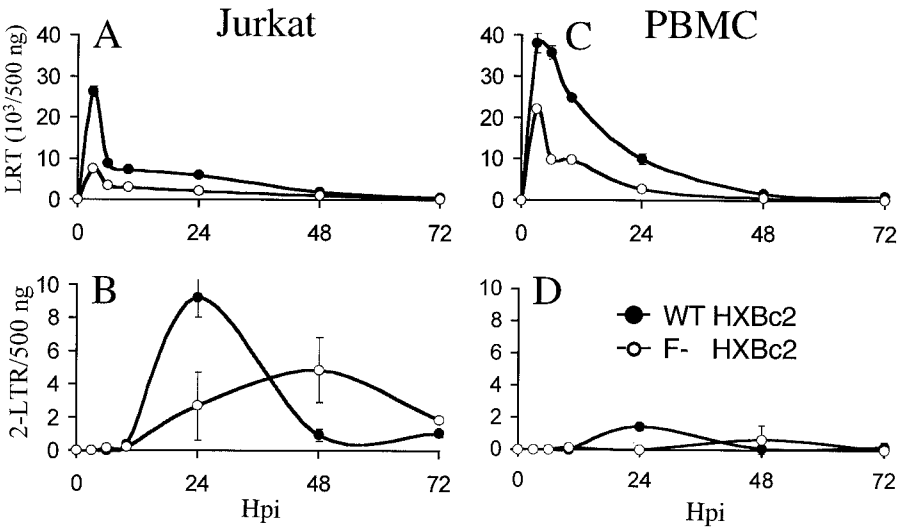

FIG. 6. F⁻ HIV-1_{HXBc2} supports wild-type level of 2-LTR circle formation in different cell types. (A) Jurkat cells infected with wild-type (WT) HIV-1_{HXBc2} (●) or F⁻ HIV-1_{HXBc2} (○) virus were lysed at the indicated times, and 500 ng of total cellular DNA was assayed for total HIV-1 cDNA by RQ-PCR. (B) Cell lysates from panel A were analyzed for 2-LTR circle levels. (C) PBMC infected and processed as indicated for Jurkat cells in panel A. (D) 2-LTR circle levels of wild-type and F⁻ HIV-1_{HXBc2} in PBMC. Other labeling is the same as in Fig. 5.

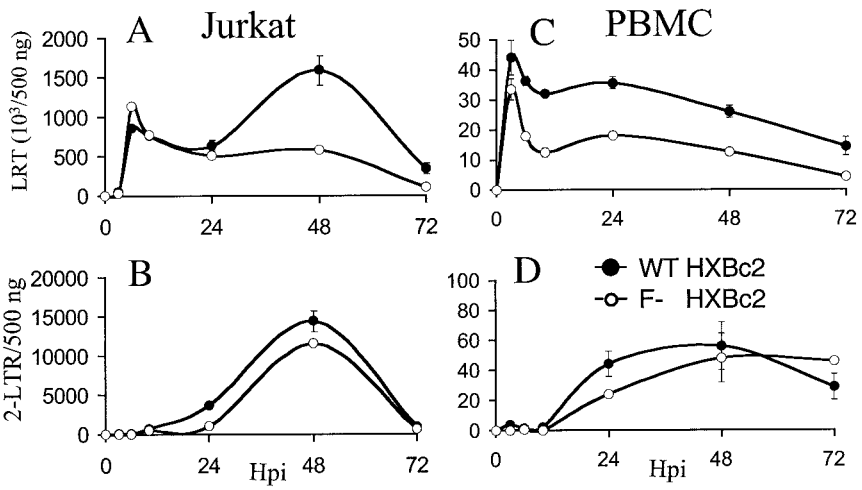

FIG. 7. Wild-type and F⁻ HIV-1_{HXBc2} VSV-G pseudotypes form similar levels of 2-LTR circles in Jurkat cells and PBMC. (A) Jurkat cells infected with VSV-G-pseudotyped wild-type (WT) and F⁻ HIV-1_{HXBc2} viruses were lysed at the indicated times, and 500 ng of total cellular DNA was assayed for total HIV-1 cDNA by RQ-PCR. (B) Lysates from panel A were assayed for 2-LTR circles by RQ-PCR. (C) PBMC infected with VSV-G pseudotypes were processed as described for panel A. (D) 2-LTR circle levels in PBMC infected with VSV-G pseudotypes. Other labeling is the same as in Fig. 5.

results in the previous section failed to detect a defect in F⁻ HIV-1_{HXBc2} 2-LTR circle formation relative to total cDNA synthesis in Jurkat cells or PBMC (Fig. 6 and 7; Table 1). To further probe the relationship between strain-specific sequences and flap function, wild-type and F⁻ HIV-1_{NL4-3} and HIV-1_{HXBc2} viruses were analyzed in side-by-side single-round transduction assays. Jurkat cells were infected with equal RT cpm of Env⁻ vectors carrying the bacterial CAT gene in place of *nef*, and the levels of wild-type and F⁻ virus required for 50% activity were calculated following endpoint dilution analyses of infected cell lysates in in vitro CAT assays (37).

Wild-type HIV-1_{NL4-3} was about sixfold more active than wild-type HIV-1_{HXBc2} in these assays, as about 3×10^7 RT cpm and 5×10^6 RT cpm of HIV-1_{HXBc2} and HIV-1_{NL4-3}, respectively, were required for 50% conversion. Whereas the cPPT-D mutation reduced the infectivity of HIV-1_{HXBc2} two- to threefold, it had no discernible effect on the transduction activity of HIV-1_{NL4-3} (Fig. 8). Thus, the slight nuclear import defect observed in Fig. 5 did not appear to impact the activity of F⁻ HIV-1_{NL4-3} in either spreading (Fig. 2) or single-round (Fig. 8) infection assays.

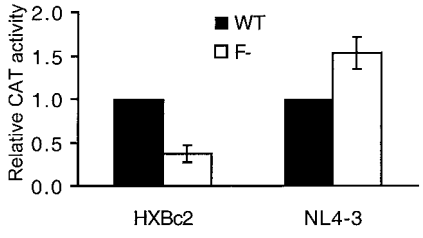

FIG. 8. Single-round infectivities of wild-type and F⁻ HIV-1_{NL4-3} and HIV-1_{HXBc2}. Levels of wild-type (WT) HIV-1_{NL4-3} and wild-type HIV-1_{HXBc2} required for 50% CAT activity, approximately 5×10^6 RT cpm and 3×10^7 RT cpm, respectively, were normalized to 1.0. The levels of F⁻ HIV-1_{NL4-3} and F⁻ HIV-1_{HXBc2} required for 50% activity are shown in comparison to their wild-type counterparts. Error bars represent the standard deviation of three independent infections.

Since Nef has been shown to play an important role in primary cell infectivity (30, 36, 45) and the HIV-1_{HXBc2} strain used in the spreading infection assays in Fig. 3 was a *vpr nef* double mutant, we next analyzed Nef-positive derivatives of wild-type and F⁻ HIV-1_{HXBc2} to determine if *nef* contributed to the strain-dependent replication phenotypes of F⁻ HIV-1_{NL4-3} (Fig. 2) and F⁻ HIV-1_{HXBc2} (Fig. 3) in PBMC.

PBMC infected with 4×10^4 RT cpm of Nef⁻ HIV-1_{HXBc2} supported peak virus growth 11 days postinfection (Fig. 9). Although Nef⁻ HIV-1_{HXBc2} replication was delayed approximately 5 days compared with its growth in Fig. 3H, we note that the two experiments used PBMC derived from different blood donors. Similar to the results in Fig. 3H, F⁻ Nef⁻ HIV-1_{HXBc2} failed to initiate a spreading infection in PBMC (Fig. 9).

Functional Nef significantly enhanced the replication of both wild-type and F⁻ HIV-1_{HXBc2} in PBMC. Whereas Nef⁺ HIV-1_{HXBc2} reached its peak growth 9 days postinfection, Nef⁺ F⁻ HIV-1_{HXBc2} displayed peak growth at 11 days postin-

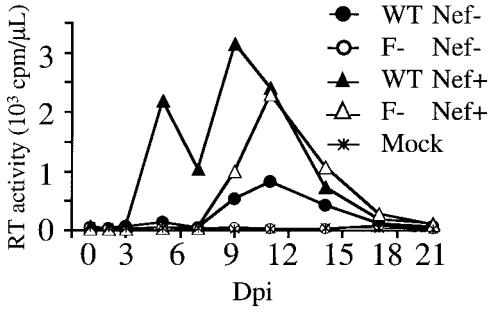

FIG. 9. Replication defect of F⁻ HIV-1_{HXBc2} in PBMC is partially restored by wild-type *nef*. PBMC infected with 4×10^4 RT cpm of Nef⁻ HIV-1_{HXBc2} (●), Nef⁻ F⁻ HIV-1_{HXBc2} (○), Nef⁺ HIV-1_{HXBc2} (▲), Nef⁺ F⁻ HIV-1_{HXBc2} (△), or supernatant from a mock transfection (×) were analyzed for RT activity at the indicated times. Dpi, days postinfection.

fection (Fig. 9). Since the results of RQ-PCR assays indicated that Nef$^-$ wild-type and F$^-$ Nef$^-$ HIV-1_{HXBc2} entered PBMC nuclei with similar efficiencies (Fig. 6 and 7; Table 1), we conclude that the *nef* defect, and not nuclear import, was primarily responsible for the spreading replication defect of Nef$^-$ F$^-$ HIV-1_{HXBc2} in PBMC (Fig. 3H and 9).

DISCUSSION

The central DNA flap is an approximately 100-base plus-strand overlap in de novo-synthesized lentiviral cDNA. Previously, it was shown that the cPPT-D mutation, which altered a total of 10 bp in the central U-box and cPPT (Fig. 1), destroyed the synthesis of the flap during reverse transcription of HIV-1_{LAI} (50). Consistent with this finding, we found that the cPPT-D mutation abolished the synthesis of the central DNA flap in HIV-1_{NL4-3} and HIV-1_{HXBc2} (Fig. 4). In stark contrast to the previous report, however, we found that F$^-$ HIV-1_{NL4-3} and F$^-$ HIV-1_{HXBc2} replicated efficiently in MT-4 cells, even when assayed at extremely low MOIs (Fig. 2C and 3C). We note that our description of efficient F$^-$ replication did not depend on the HIV-1_{NL4-3} and HIV-1_{HXBc2} strains studied here, as Dvorin and coworkers have described efficient F$^-$ HIV-1_{YU-2} and F$^-$ HIV-1_{LAI} replication under a variety of infection conditions (see the companion paper by Dvorin et al. [16a] in this issue).

Virus strain- and target cell type-dependent flap function. Our results did reveal a role for the flap in HIV-1 spreading replication, but this was highly strain and target cell type dependent (Fig. 2 and 3). F$^-$ HIV-1_{NL4-3} was basically a wild-type virus (Fig. 2). Although F$^-$ HIV-1_{HXBc2} replicated poorly in PBMC, we failed to detect a nuclear import defect under these infection conditions (Fig. 6 and 7; Table 1), and instead determined that the *nef* mutant phenotype of this strain played a large part in the observed replication defect (Fig. 9).

Since several previously reported F$^-$ vectors incorporated HIV-1_{NL4-3} sequences (16, 20, 44, 50, 51), we were somewhat surprised that our F$^-$ HIV-1_{NL4-3} vector transduced Jurkat cells as efficiently as the wild type did (Fig. 8). One possible explanation may be the genome sizes of the vectors in the different studies. Since most of HIV-1_{NL4-3} was removed from the previously analyzed vector constructs, it is possible that sequences present in our nearly full-length HIV-1_{NL4-3} vector helped to counteract the loss of the central DNA flap. We speculate that minor discontinuities observed throughout the F$^-$ HIV-1_{NL4-3} plus strand (Fig. 4, lane 5) could potentially fulfill this role. Although the cPPT-D mutation reduced the single-round infectivity of our HIV-1_{HXBc2} vector two- to threefold, we emphasize that this did not correlate with reduced nuclear import (Fig. 6 and Table 1). We speculate that reduced cDNA synthesis (Fig. 6A) and/or delayed nuclear import (Fig. 6B) may account for the observed reduction in F$^-$ HIV-1_{HXBc2} activity in single-round infections (Fig. 8). A delay in 2-LTR circle formation in infected HeLa cells was previously noted for a small F$^-$ HIV-1_{NL4-3} vector (20).

Single-round infectivity versus spreading HIV-1 replication. Our finding that F$^-$ HIV-1_{HXBc2} was two- to threefold defective in single-round transduction assays (Fig. 8) agrees with numerous previous reports that the flap imparted an infection advantage of between 2- and 10-fold on single-round HIV-1 vectors (16, 20, 39, 40, 44, 50, 51). However, we emphasize that this slight defect in single-round infectivity did not correlate with a severe defect in spreading HIV-1 replication (Fig. 3D).

We previously determined by endpoint dilution that HIV-1_{NL4-3} lacking functional integrase was approximately 58,000-fold defective in its ability to initiate a spreading infection in MT-4 cells (37). Yet, when analyzed in bulk cultures infected at a relatively high MOI, growth of the integrase-negative HIV-1_{NL4-3} was delayed only about 1 week compared with the wild-type virus (37). Considering these results, one would predict that mutants displaying just 2- to 10-fold defects in single-round infectivity assays, like the F$^-$ HIV-1_{HXBc2} strain studied here, would spread with close to wild-type efficiency in bulk-infected cell cultures (Fig. 3 and 9).

Although the flap can influence the single-round transduction activity of certain HIV-1 vectors as much as 10-fold and is therefore likely an important regulatory sequence for lentivirus-based gene therapy vectors, the results presented here cast doubt on the prior claim that the central DNA flap is an essential determinant of preintegration complex nuclear import and spreading HIV-1 infectivity (50). Experiments aimed at elucidating the major player(s) in the nuclear import of HIV-1 preintegration complexes in nondividing and dividing cells are currently under way in our laboratory.

ACKNOWLEDGMENTS

We thank D. Gabuzda, H. Göttlinger, and J. Sodroski for gifts of plasmid DNAs and valuable discussions and J. D. Dvorin and M. H. Malim for sharing results prior to publication.

This work was supported by NIH grants AI39394 (A.E.), AI45313 (A.E.), and AI28691 (Center for AIDS Research); by a gift from the G. Harold and Leila Y. Mathers Charitable Foundation (A.E.); and by the Japanese Foundation for AIDS Prevention (N.N.).

REFERENCES

1. **Adachi, A., H. E. Gendelman, S. Koenig, T. Folks, R. Willey, A. Rabson, and M. A. Martin.** 1986. Production of acquired immunodeficiency syndrome-associated retrovirus in human and nonhuman cells transfected with an infectious molecular clone. J. Virol. **59:**284–291.
2. **Bouyac-Bertoia, M., J. D. Dvorin, R. A. Fouchier, Y. Jenkins, B. E. Meyer, L. I. Wu, M. Emerman, and M. H. Malim.** 2001. HIV-1 infection requires a functional integrase nuclear localization signal. Mol. Cell **7:**1025–1035.
3. **Bowerman, B., P. O. Brown, J. M. Bishop, and H. E. Varmus.** 1989. A nucleoprotein complex mediates the integration of retroviral DNA. Genes Dev. **3:**469–478.
4. **Brown, H. E. V., H. Chen, and A. Engelman.** 1999. Structure-based mutagenesis of the human immunodeficiency virus type 1 DNA attachment site: effects on integration and cDNA synthesis. J. Virol. **73:**9011–9020.
5. **Bukovsky, A. A., T. Dorfman, A. Weimann, and H. G. Göttlinger.** 1997. Nef association with human immunodeficiency virus type 1 virions and cleavage by the viral protease. J. Virol. **71:**1013–1018.
6. **Bukrinsky, M. I., N. Sharova, M. P. Dempsey, T. L. Stanwick, A. G. Bukrinskaya, S. Haggerty, and M. Stevenson.** 1992. Active nuclear import of human immunodeficiency virus preintegration complexes. Proc. Natl. Acad. Sci. USA **89:**6580–6584.
7. **Butler, S. L., M. S. Hansen, and F. D. Bushman.** 2001. A quantitative assay for HIV DNA integration in vivo. Nat. Med. **7:**631–634.
8. **Charneau, P., M. Alizon, and F. Clavel.** 1992. A second origin of DNA plus-strand synthesis is required for optimal human immunodeficiency virus replication. J. Virol. **66:**2814–2820.
9. **Charneau, P., and F. Clavel.** 1991. A single-stranded gap in human immunodeficiency virus unintegrated linear DNA defined by a central copy of the polypurine tract. J. Virol. **65:**2415–2421.
10. **Charneau, P., G. Mirambeau, P. Roux, S. Paulous, H. Buc, and F. Clavel.** 1994. HIV-1 reverse transcription. A termination step at the center of the genome. J. Mol. Biol. **241:**651–662.
11. **Chen, H., and A. Engelman.** 2001. Asymmetric processing of human immunodeficiency virus type 1 cDNA in vivo: implications for functional end coupling during the chemical steps of DNA transposition. Mol. Cell. Biol. **21:**6758–6767.

12. **Chen, H., S.-Q. Wei, and A. Engelman.** 1999. Multiple integrase functions are required to form the native structure of the human immunodeficiency virus type 1 intasome. J. Biol. Chem. **274:**17358–17364.
13. **Cimarelli, A., S. Sandin, S. Hoglund, and J. Luban.** 2000. Rescue of multiple viral functions by a second-site suppressor of a human immunodeficiency virus type 1 nucleocapsid mutation. J. Virol **74:**4273–4283.
14. **Coffin, J. M.** 1996. Retroviridae: the viruses and their replication, p. 1767–1848. *In* B. N. Fields, D. M. Knipe, and P. M. Howley (ed.), Fields virology. Lippincott-Raven Publishers, Philadelphia, Pa.
15. **Cullen, B. R.** 2001. Journey to the center of the cell. Cell **105:**697–700.
16. **Dardalhon, V., B. Herpers, N. Noraz, F. Pflumio, D. Guetard, C. Leveau, A. Dubart-Kupperschmitt, P. Charneau, and N. Taylor.** 2001. Lentivirus-mediated gene transfer in primary T cells is enhanced by a central DNA flap. Gene Ther. **8:**190–198.

16a. **Dvorin, J. D., P. Bell, G. G. Maul, M. Yamashita, M. Emerman, and M. H. Malim.** 2002. Reassessment of the roles of integrase and the central DNA flap in human immunodeficiency virus type 1 nuclear import. J. Virol. **76:**12087–12096.

17. **Engelman, A., G. Englund, J. M. Orenstein, M. A. Martin, and R. Craigie.** 1995. Multiple effects of mutations in human immunodeficiency virus type 1 integrase on viral replication. J. Virol. **69:**2729–2736.
18. **Farnet, C. M., and W. A. Haseltine.** 1990. Integration of human immunodeficiency virus type 1 DNA in vitro. Proc. Natl. Acad. Sci. USA **87:**4164–4168.
19. **Fisher, A. G., E. Collati, L. Ratner, R. C. Gallo, and F. Wong-Staal.** 1985. A molecular clone of HTLV-III with biological activity. Nature **316:**262–265.
20. **Follenzi, A., L. E. Ailles, S. Bakovic, M. Guena, and L. Naldini.** 2000. Gene transfer by lentiviral vectors is limited by nuclear translocation and rescued by HIV-1 pol sequences. Nat. Genet. **25:**217–222.
21. **Fouchier, R. A., and M. H. Malim.** 1999. Nuclear import of human immunodeficiency virus type-1 preintegration complexes. Adv. Virus Res. **52:**275–299.
22. **Goff, S. P.** 2001. Intracellular trafficking of retroviral genomes during the early phase of infection: viral exploitation of cellular pathways. J. Gene Med. **3:**517–528.
23. **Göttlinger, H. G., T. Dorfman, E. A. Cohen, and H. A. Haseltine.** 1993. Vpu protein of human immunodeficiency virus type 1 enhances the release of capsids produced by gag gene constructs of widely divergent retroviruses. Proc. Natl. Acad. Sci. USA **90:**7381–7385.
24. **Hatziioannou, T., and S. P. Goff.** 2001. Infection of nondividing cells by Rous sarcoma virus. J. Virol. **75:**9526–9531.
25. **Helseth, E., M. Kowalski, D. Gabuzda, U. Olshevsky, W. Haseltine, and J. Sodroski.** 1990. Rapid complementation assays measuring replicative potential of human immunodeficiency virus type 1 envelope glycoprotein mutants. J. Virol. **64:**2416–2420.
26. **Hungnes, O., E. Tjotta, and B. Grinde.** 1991. The plus strand is discontinuous in a subpopulation of unintegrated HIV-1 DNA. Arch. Virol. **116:**133–141.
27. **Hungnes, O., E. Tjotta, and B. Grinde.** 1992. Mutations in the central polypurine tract of HIV-1 result in delayed replication. Virology **190:**440–442.
28. **Ilyinski, P. O., and R. C. Desrosiers.** 1998. Identification of a sequence element immediately upstream of the polypurine tract that is essential for replication of simian immunodeficiency virus. EMBO J. **17:**3766–3774.
29. **Julias, J. G., A. L. Ferris, P. L. Boyer, and S. H. Hughes.** 2001. Replication of phenotypically mixed human immunodeficiency virus type 1 virions containing catalytically active and catalytically inactive reverse transcriptase. J. Virol. **75:**6537–6546.
30. **Kawano, Y., Y. Tanaka, N. Misawa, R. Tanaka, J.-I. Kira, T. Kimura, M. Fukushi, K. Sano, T. Goto, M. Nakai, T. Kobayashi, N. Yamamoto, and Y. Koyanagi.** 1997. Mutational analysis of human immunodeficiency virus type 1 (HIV-1) accessory genes: requirement of a site in the *nef* gene for HIV-1 replication in activated $CD4^+$ T cells in vitro and in vivo. J. Virol. **71:**8456–8466.
31. **Lewin, S. R., M. Vesanen, L. Kostrikis, A. Hurley, M. Duran, L. Zhang, D. D. Ho, and M. Markowitz.** 1999. Use of real-time PCR and molecular beacons to detect virus replication in human immunodeficiency virus type 1-infected individuals on prolonged effective antiretroviral therapy. J. Virol. **73:**6099–6103.
32. **Lewis, P. F., and M. Emerman.** 1994. Passage through mitosis is required for oncoretroviruses but not for the human immunodeficiency virus. J. Virol. **68:**510–516.
33. **Lewis, P., M. Hensel, and M. Emerman.** 1992. Human immunodeficiency virus infection of cells arrested in the cell cycle. EMBO J. **11:**3053–3058.
34. **Mattaj, I. W., and L. Englmeier.** 1998. Nucleocytoplasmic transport: the soluble phase. Annu. Rev. Biochem. **67:**265–306.
35. **Meyers, G., S. Wain-Hobson, B. Korber, R. F. Smith, and G. N. Pavlakis.** 1993. Human retroviruses and AIDS. A compilation and analysis of nucleic acid and amino acid sequences. Theoretical Biology and Biophysics Group, Los Alamos National Laboratory, Los Alamos, N.Mex.
36. **Miller, M. D., M. T. Warmerdam, I. Gaston, W. C. Greene, and M. B. Feinberg.** 1994. The human immunodeficiency virus-1 *nef* gene product: a positive factor for viral infection and replication in primary lymphocytes and macrophages. J. Exp. Med. **179:**101–113.
37. **Nakajima, N., R. Lu, and A. Engelman.** 2001. Human immunodeficiency virus type 1 replication in the absence of integrase-mediated DNA recombination: definition of permissive and nonpermissive T-cell lines. J. Virol. **75:**7944–7955.
38. **O'Doherty, U., W. J. Swiggard, and M. H. Malim.** 2000. Human immunodeficiency virus type 1 spinoculation enhances infection through virus binding. J. Virol. **74:**10074–10080.
39. **Park, F., and M. A. Kay.** 2001. Modified HIV-1 based lentiviral vectors have an effect on viral transduction efficiency and gene expression in vitro and in vivo. Mol. Ther. **4:**164–173.
40. **Parolin, C., B. Taddeo, G. Palu, and J. Sodroski.** 1996. Use of cis- and trans-acting viral regulatory sequences to improve expression of human immunodeficiency virus vectors in human lymphocytes. Virology **222:**415–422.
41. **Peden, K., M. Emerman, and L. Montagnier.** 1991. Changes in growth properties on passage in tissue culture of viruses derived from infectious molecular clones of $HIV\text{-}1_{LAI}$, $HIV\text{-}1_{MAL}$, and $HIV\text{-}1_{ELI}$. Virology **185:**661–672.
42. **Reil, H., A. A. Bukovsky, H. R. Gelderblom, and H. G. Göttlinger.** 1998. Efficient HIV-1 replication can occur in the absence of the viral matrix protein. EMBO J. **17:**2699–2708.
43. **Roe, T., T. C. Reynolds, G. Yu, and P. O. Brown.** 1993. Integration of murine leukemia virus DNA depends on mitosis. EMBO J. **12:**2099–2108.
44. **Sirven, A., F. Pflumio, V. Zennou, M. Titeux, W. Vainchenker, L. Coulombel, A. Dubart-Kupperschmitt, and P. Charneau.** 2000. The human immunodeficiency virus type-1 central DNA flap is a crucial determinant for lentiviral vector nuclear import and gene transduction of human hematopoietic stem cells. Blood **96:**4103–4110.
45. **Spina, C. A., T. J. Kwoh, M. Y. Chowers, J. C. Guatelli, and D. D. Richman.** 1994. The importance of *nef* in the induction of human immunodeficiency virus type 1 replication from primary quiescent CD4 lymphocytes. J. Exp. Med. **179:**115–123.
46. **Wei, S-Q., K. Mizuuchi, and R. Craigie.** 1997. A large nucleoprotein assembly at the ends of the viral DNA mediates retroviral DNA integration. EMBO J. **16:**7511–7520.
47. **Weinberg, J. B., T. J. Matthews, B. R. Cullen, and M. H. Malim.** 1991. Productive human immunodeficiency virus type 1 (HIV-1) infection of nonproliferating human monocytes. J. Exp. Med. **174:**1477–1482.
48. **Yee, J.-K., A. Miyanohara, P. LaPort, K. Bouic, J. C. Burns, and T. Friedmann.** 1994. A general method for the generation of high-titer, pantropic retroviral vectors: highly efficient infection of primary lymphocytes. Proc. Natl. Acad. Sci. USA **91:**9564–9568.
49. **Yuan, B., X. Li, and S. P. Goff.** 1999. Mutations altering the Moloney murine leukemia virus p12 Gag protein affect virion production and early events of the virus life cycle. EMBO J. **18:**4700–4710.
50. **Zennou, V., C. Petit, D. Guetard, U. Nerhbass, L. Montagnier, and P. Charneau.** 2000. HIV-1 genome nuclear import is mediated by a central DNA flap. Cell **101:**173–185.
51. **Zennou, V., C. Serguera, C. Sarkis, P. Colin, E. Perret, J. Mallet, and P. Charneau.** 2001. The HIV-1 DNA flap stimulates HIV vector-mediated cell transduction in the brain. Nat. Biotechnol. **19:**446–450.